energies

MDPI

Article

Immobilization of Alcohol Dehydrogenase, Acetaldehyde Lyase, and NADH Oxidase for Cascade Enzymatic Conversion of Ethanol to Acetoin

Xue-Yong Li [1,†], Jia-Ying Huang [1,†], Qiang Zhou [1], Yuan-Yuan Xu [1], Ponnandy Prabhu [2,*] and Ye-Wang Zhang [1,*]

[1] School of Pharmacy, Jiangsu University, Zhenjiang 212013, China; a1124976905@163.com (X.-Y.L.); huangjiaying98@yeah.net (J.-Y.H.); zhouqiangyouxiang@yeah.net (Q.Z.); xuyuanyuanmail@yeah.net (Y.-Y.X.)
[2] Department of Chemical Engineering, University of Michigan, Ann Arbor, MI 48109, USA
* Correspondence: prabhup@umich.edu (P.P.); zhangyewang@ujs.edu.cn (Y.-W.Z.); Tel.: +86-511-85038201 (Y.-W.Z.)
† These authors contributed equally to this work.

Abstract: Acetoin, a four-carbon hydroxyl-keto compound, is used in the food, pharmaceutical, and chemical industries. The cascade enzymatic production is considered a promising and efficient method to produce acetoin. However, the stability and compatibility of the enzymes under the same catalytic conditions are challenges that need to be resolved. In this work, alcohol dehydrogenase, acetaldehyde lyase, and NADH oxidase were selected to work at the same conditions to efficiently convert ethanol into acetoin. These three enzymes were immobilized on epoxy-modified magnetic nanomaterials to obtain highly stable biocatalysts. The stability and the immobilization conditions, including temperature, pH, enzyme–carrier ratio, and immobilization time, were optimized to obtain the immobilized enzymes with a high catalytic activity. The cascade reactions catalyzed by the immobilized enzymes yielded a high conversion of 90%, suggesting that the use of immobilized enzymes is a promising way to produce acetoin.

Keywords: immobilization; NADH oxidase; acetaldehyde lyase; alcohol dehydrogenase; acetoin; cascade enzymatic reactions

Citation: Li, X.-Y.; Huang, J.-Y.; Zhou, Q.; Xu, Y.-Y.; Prabhu, P.; Zhang, Y.-W. Immobilization of Alcohol Dehydrogenase, Acetaldehyde Lyase, and NADH Oxidase for Cascade Enzymatic Conversion of Ethanol to Acetoin. *Energies* **2022**, *15*, 4242. https://doi.org/10.3390/en15124242

Academic Editors: Fernando Rubiera González and Covadonga Pevida García

Received: 26 December 2021
Accepted: 7 June 2022
Published: 9 June 2022

1. Introduction

Due to their large specific surface area, superparamagentism, easy preparation, and so on, Fe_3O_4 nanoparticles show great potential for biomedical applications [1–3]. For example, they are widely used as a carrier for the immobilization of protein molecules [4]. However, magnetic nanoparticles are prone to aggregation and have few reactive groups on the surface. The surface modification of magnetic materials could largely avoid the above problems and achieve more efficient immobilization of protein molecules [1]. Epoxy groups react with large molecules such as enzymes, proteins, and nucleic acids due to their high reactivity. In addition, epoxy groups show a lower loss of enzyme activity compared to amino and cyano [2]. Therefore, epoxy group modified magnetic nanoparticles are considered as good immobilization carriers and are widely used for enzyme immobilization [4].

Acetoin (3-hydroxy-2-butanone), as an important compound, has various applications in food [5], pharmaceutical industries [6], and chemical synthesis [7]. It could be used for beer fermentation as a flavor enhancer [8], for the synthesis of an essential active alkaloid ligustrazine as a precursor [9], and for the stabilization of alkoxide as a stabilizer reagent [10]. In addition, acetoin is recognized as a flavor and aroma agent by the US Food and Drug Administration, owing to improving the taste and safety of food. Although acetoin exists in fruits and vegetables, the production could not meet the market demand [11]. At present, it is mainly produced by diacetyl chemical reduction, the selective oxidation of butanedione, alkaline hydrolysis, and the hydrogenation of acetaldehyde. However,

these methods suffer difficulties including active metals reduction, concentrated sulfuric acid oxidation, and equipment corrosion caused by aldehydes [11]. Furthermore, chemical production undoubtedly increases the burden of environmental pollution and the difficulty of product separation [12].

As energy consumption and environmental pollution are increasingly concerned, the biotransformation production of acetoin has attracted extensive attention [13]. The wild and engineered strains, including *Enterobacter*, *Klebsiella*, *Serratia*, *Corynebacterium glutamicum*, *Saccharomyces cerevisiae*, and *Bacillus*, have been investigated for the fermentative production of acetoin [14–18]. However, acetoin is an intermediate in the 2, 3-butanediol metabolic pathway, which means that the main product of most bacterial strains is 2, 3-butanediol. Thus, different metabolic engineering strategies are required to redistribute the carbon flux to acetoin [19]. For example, acetoin production increased to 0.63 g/g with crude glycerol as the carbon source by regulating metabolic pathways [20]. Although a high titer of acetoin has been achieved in fermentative production, the various nutrients and raw materials used for strain growth during fermentation make separating the product a challenge.

Recently, several pieces of research about the enzymatic production of acetoin have been published, including the biosynthetic pathways of acetoin and the relevant key enzymes, various strategies for biological production of acetoin, and the advantages and disadvantages of the different approaches [20]. The purified enzymes used to convert ethanol to high-value acetoin seem to be a better choice because the enzymatic method can effectively overcome the difficulties in the methods mentioned above for acetoin production. Zhang et al. reported the use of purified enzymes for the conversion of ethanol to acetoin [21]. However, there are still a few issues that need to be addressed urgently. The toxic effect of the substrate acetaldehyde leading to a significant loss of enzyme activity occurred when the conversion of acetylene was catalyzed by acetaldehyde lyase (FLS). The compatibility and catalytic efficiency of these enzymes under the same catalytic conditions are also a challenge that need to be addressed. Meanwhile, the application of the purified enzymes is also hampered by the operational stability and the reuse of the enzymes. Immobilization is considered as an effective strategy to improve enzyme stability and multi-enzyme cascades compatibility.

In fact, previous researchers have attempted to catalyze the specific conversion of lactic acid to the value-added compound ethylene coupling via a three-step process in a four-enzyme cascade reaction [22]. Immobilization is the method to immobilize the soluble enzyme and make it an insoluble form and could be used and recycled in many industrial productions. The enzyme stability under the reaction conditions could be notably improved by fixing onto a specific carrier [23]. The immobilized enzymes can be recovered and reused, and often maintain a high activity for a considerable operation time. Likewise, using enzymes in a heterogeneous form brings advantages, such as simplified downstream processing or continuous processing operations. The immobilized enzymes display a wide working-pH and temperature range, increasing the compatibility of the multi-enzymes [24].

In this work, three well-compatible enzymes were selected and immobilized to synthesize acetoin. The alcohol dehydrogenase (ADH) was used to convert ethanol into acetaldehyde, thus reducing the damage due to the high initial concentration of acetaldehyde to the enzyme. The NADH oxidase (NOX) is designed to decrease the consumption of the expensive cofactors and to avoid the product inhibition caused by NADH accumulation. The FLS for the conversion of acetoin was aimed to avoid the loss of catalytic activity because of the amassment of acetaldehyde. Immobilization was further employed to improve the compatibility as well as the stability of these three enzymes. Finally, the immobilized enzyme system was able to efficiently convert ethanol to acetoin with a conversion of 90%.

2. Materials and Methods

2.1. Materials

Escherichia coli (BL21) was from Sangon (Shanghai, China). Reduced nicotinamide adenine dinucleotide, β-nicotinamide adenine dinucleotide (NAD+), dithiothreitol, flavin

adenine dinucleotide disodium salt hydrate, 2-[4-(2-hydroxyethyl) piperazin-1-yl] ethane sulfonic acid (HEPES), γ-glycidoxypropyl trimethoxy silane (GPS), and bovine serum albumin were purchased from Sigma-Aldrich (St. Louis, MO, USA). Ferric chloride hexahydrate ($FeCl_3 \cdot 6H_2O$), ferrous sulfate heptahydrate ($FeSO_4 \cdot 7H_2O$), sodium silicate ($Na_2SiO_3 \cdot 9H_2O$), tetraethyl orthosilicate (TEOS), and NaOH, ethanol, acetaldehyde were obtained from Sinopharm Chemical Reagent Co., Ltd. (Shanghai, China). Ni-NTA chromatographic columns were bought from Sangon Biotech (Shanghai, China). Acetoin, isopropyl-β-D-thiogalactopyranoside (IPTG), yeast extract, and kanamycin were purchased from Aladdin Biotechnology Co., Ltd. (Shanghai, China). Unless otherwise noted, all reagents and chemicals were analytic or biological grade.

2.2. The Enzyme Assays

ADH activity: The specific activity of ADH was determined by spectrophotometry with ethanol as the substrate [25]. The reaction mixture consisting of 50 mM Tris-HCl (pH 9.0), 5 mM Mg^{2+}, 3 mM NAD^+,10 mM ethanol, and 50 $\mu g \cdot mL^{-1}$ was carried out at 25 °C for 5 min. The absorbance of the solution at 340 nm was measured, and NADH concentration was calculated. One unit of ADH is defined as the amount of enzyme required to produce 1 μmol of NADH per minute.

NOX activity: The specific activity of NOX was determined by spectrophotometry according to previous research [26]. The reaction solution for determining the activity of NOX contained 10 μM FAD, 100 μM NADH, 1 mM dithiothreitol (DTT), 50 mM phosphate buffer (pH 7.0), and 10 $\mu g \cdot mL^{-1}$ Nox. After 1 min of enzymatic reaction at 25 °C, the NADH concentration was calculated using the relationship between the absorbance at 340 nm and NADH concentration. One unit of NOX is defined as the quantity of enzyme needed to reduce 1 μmol NADH per minute.

FLS activity: The reaction mixture consisting of 50 mM HEPES (pH 8.0) buffer, 1mM Mg^{2+}, 0.1 mM thiamine pyrophosphate (TPP), 10 mM acetaldehyde, and 10 $mg \cdot ml^{-1}$ FLS was carried out at 25 °C for 30 min. The reaction solution was immediately transferred into the boiling water for 5 min to quench the reaction, and the acetoin concentration in the solution was determined by the Voges–Proskauer reaction [27]. The 0.1 mL resulting solution, 0.3 mL creatine (0.5%, *w*/*v*), 0.3 mL 1-naphthol (5%, *w*/*v*), and 0.3 mL sodium hydroxide (5%, *w*/*v*) were added to a 4 mL test tube and bathed in water at 30 °C for 30 min. The absorbance of the solution at 520 nm was measured, and the acetoin concentration was calculated according to the corresponding relationship between the absorbance and acetoin concentration. One unit of FLS activity was defined as the amount of enzyme required to produce 1 μmol acetoin per minute.

The immobilized enzyme activity: the amount of free enzyme is converted into an equivalent amount of immobilized enzyme, and the immobilized enzyme activity was determined according to the free enzyme assay method.

2.3. Synthesis of Fe_3O_4@SiO_2-Epoxy Nanoparticles

Epoxy-modified magnetic Fe_3O_4 materials were synthesized according to previous studies [25]. Briefly, 0.08 mol $FeCl_3 \cdot 6H_2O$ and 0.04 mol $FeCl_2 \cdot 4H_2O$ were dissolved in aqueous, then NaOH aqueous solution (1.5 M) was added dropwise, and the mixture was stirred for 2 h under a nitrogen flow (20 mL/min). Fe_3O_4 nanoparticles were collected using a magnetic field and washed 5 times with deionized water. The Fe_3O_4 nanoparticles were dried at 60 °C under vacuum.

The solution containing 1 g Fe_3O_4 and 300 mL ethanol (80%, *v*/*v*) was dispersed by ultrasound for 10 min. Then, 20 mL ammonia water was added under a nitrogen flow at room temperature, followed by 3 mL TEOS (ethyl orthosilicate), and the mixture was stirred vigorously for 5 h. The Fe_3O_4 nanoparticles coated with silica were washed several times with ethanol and water, and vacuum-dried at 60 °C.

The solution containing 2 g Fe_3O_4@SiO_2 and 98 mL toluene was sonicated for 30 min, and 0.3 mL Et_3N and 2 mL GPS were added into the system. The modification of epoxy

groups was carried out at reflux and stirred at 115 °C in N_2 atmosphere for 3 h. The resulting epoxy functionalized nanoparticles were washed several times with acetone and dried in a vacuum at 60 °C.

2.4. Expression and Purification of Recombinant Enzymes

The gene of ADH, FLS, and NOX was cloned into plasmid pET28a, respectively [26–28]. The three recombinant plasmids were introduced into *E. coli* and incubated in Luria-Bertani (LB) broth with 50 μg·mL^{-1} of kanamycin at 37 °C. When the OD_{600} of the medium reached at a certain value (ADH and NOX for 0.8, FLS for 1.0), different concentrations of isopropyl-β-D-thiogalactopyranoside (IPTG) were added to the medium (ADH and NOX for 1.0, FLS for 0.1). The FLS was induced at 20 °C for 24 h. The ADH and NOX were induced at 15 °C for 8 h, respectively. The cells were harvested by centrifugation at 3156× *g* for 15 min at 4 °C. Then cells were resuspended in buffer and disrupted by ultrasonication in an ice-water bath. To remove the cell debris, the cell lysate was centrifuged at 6134× *g* for 10 min, and the soluble fraction was then purified with the Ni-NTA resin to obtain the purified enzymes.

2.5. Immobilization of Enzymes

ADH immobilization: the mixture containing 100 μg of enzyme and 10 mg of epoxy-modified magnetic nanomaterial was gently shaken to immobilize enzymes in pH 8.0 HEPES buffer (50 mM) at 25 °C for 1 h.

FLS immobilization: the mixture comprising 100 μg of enzyme and 10 mg of epoxy-modified magnetic nanomaterial was gently shaken to immobilize enzymes in pH 7.0 phosphate buffer (50 mM) at 20 °C for 2 h.

NOX immobilization: the mixture including 100 μg of enzyme and 10 mg of epoxy-modified magnetic nanomaterial was gently shaken to immobilize enzymes in pH 8.0 HEPES buffer (50 mM) at 15 °C for 2 h.

The immobilization conditions were investigated: temperature (4–40 °C), pH (6–11), time (0.5–8 h), and the ratio of protein to carrier (5–40 mg·g^{-1}). The collected particles were washed with 1mL pH 8.0 HEPES buffer 3 times. The protein concentration of the solution was measured with the Bradford method using bovine serum albumin as standard [29]. The immobilization yield (Y) and efficiency (E) were calculated according to Equation (1) and Equation (2).

$$Y = (A_0 - A_1)/A_0 \quad (1)$$

$$E = (B_0 - B_1)/B_0 \quad (2)$$

A_0: the amount of initial protein; A_1: the amount of protein in supernatant; B_0: total enzyme activity; B_1 = the enzyme activity of the supernatant.

2.6. The Synthesis of Acetoin with Immobilized Enzymes

Acetoin production was carried out in the reaction mixture containing 50 mM HEPES buffer (pH 8.0), 1 mM NAD^+, immobilized enzymes (0.1 mg·mL^{-1} ADH, 0.2 mg·mL^{-1} FLS, and 0.1 mg·mL^{-1} NOX), 0.1 mM TPP, 1 mM Mg^{2+}, 1 mM DTT, and 10 mM ethanol. The reaction was conducted at 35 °C. Aliquots of the reaction solution were drawn at regular intervals and the acetoin concentration was determined by the Voges–Proskauer reaction.

2.7. The Reusability of Immobilized Cascade Enzymes

The reusability of the immobilized cascade enzymes was assessed by using them repeatedly. The immobilized enzymes were reacted 6 times at 50 mM HEPES buffer (pH 8.0) and 35 °C. The activity of the cascade enzymes in the first cycle was assumed to be 100% and the remaining activity of each enzyme was calculated.

3. Results and Discussion

3.1. The Selection of Cascade Enzymes and the Enzyme Assays

The most important aspect of cascade reactions is the catalytic efficiency of multiple enzymes under the same catalytic conditions [30–33]. The use of enzymes in cascade reactions is completely different from the non-simultaneous use of enzymes. The latter can be used with maximum catalytic efficiency under the most favorable conditions. Under different catalytic conditions, enzymes have various abilities to catalyze and can even produce opposite reactions. For example, ADH achieves the conversion of alcohols to aldehydes under alkaline conditions, and vice versa under acidic conditions. Therefore, it is important to select enzymes that are compatible with each other for the cascade reaction. Based on their kinetic parameters, optimal pH, and temperature, three enzymes with good compatibility and high catalytic activity were selected [26–28]. As summarized in Table 1, these three enzymes have a similar optimal pH and temperature, as well as a high catalytic activity. Notably, the kinetic parameters of aldehyde ligases were difficult to measure due to the dramatic loss of enzyme activity from high concentrations of aldehyde-containing substrates. This is also an important reason why we constructed the cascade enzyme reactions. After enzyme expression and purification, the free enzyme activities of ADH, FLS, and NOX under the respective catalytic conditions were 5.3, 1.4, and 124 U·mg^{-1}.

Table 1. Biochemical and kinetic properties of NOX, ADH, and FLS from various organisms.

Enzyme	Organism	V_{max} (U·mg^{-1})	K_m (μM)	T_{opt} (°C)	pH_{opt}	Reference
NOX	*Lactobacillus Rhamnosus*	263	5.8	50	5.5	[34]
	Lactobacillus rhamnosus	NA	24	40	6.0	[35]
	Clostridium Aminovalericum	119	19.2	40	6.0	[36]
	Streptococcus Mutans	154.3	57.7	35	7.0	[26]
	Streptococcus Pyogenes	344	27.0	55	7.0	[33]
	Thermococcus Kodakaraensis	83.1	24.2	75	8.0	[31]
ADH	*Euglena Gracilis*	11.7	3.2	NA	7.0	[32]
	NA	10.64	0.37	25	8.0	[27]
	Lignocellulosic	4.33	3.15	30	6.0	[37]
	Candida Parapsilosis	NA	NA	35	4.5	[38]
	Natronomonas pharaonis	0.36	3.4×10^5	70	9.0	[39]
	Haloarcula Marismortui	1.6	5.1	60	NA	[40]
FLS	*Pseudomonas fluorescens*	NA	NA	NA	9.5	[41]
	Pseudomonas fluorescens	NA	NA	35	NA	[9]
	Pseudomonas fluorescens	NA	NA	NA	8.0	[28]

3.2. The Effects of Temperature and pH on the Immobilization

The linkage between the enzyme and the substrate relies mainly on the ring-opening of the epoxide group, which forms a covalent bond with the amino group on the amino acid side chain on the protein. The epoxide group would also react with the carboxyl groups or other groups on the amino acid side chains on the protein. However, it accounted for a small proportion and required acidic or other specific conditions [42]. The increase in temperature improved the reaction activity and even raised the stability of the enzyme, forming a multiple site immobilization. However, the rise in temperature also led to a loss of enzyme activity due to the denaturation and inactivation of the protein. Therefore, the effect of temperature on enzyme immobilization has been investigated to retain the maximum enzyme activity (Figure 1). As the temperature increased, the immobilization yields of ADH and NOX increased, while the immobilization efficiency decreased. This was consistent with the theory described in the previous section. In contrast, the immobilization efficiency of FLS had almost no obvious change, which may be related to its own higher thermal stability [41]. Notably, compared with FLS, the immobilization efficiency of ADH and NOX was lower. It may be caused by two main reasons, including an increased resistance to substrate transfer due to the immobilization of the enzyme on the surface of

the carrier, and a loss of activity owing to the bonding of the amino group to the carrier near the active pocket. Considering the immobilization efficiency and immobilization yield, the respective appropriate temperatures (ADH for 15 °C, NOX for 25 °C, FLS for 20 °C) were finally chosen to maintain the enzyme activity. Correspondingly, the immobilization efficiency of FLS, ADH, and NOX is 78.2, 42.3, and 13.9%, respectively.

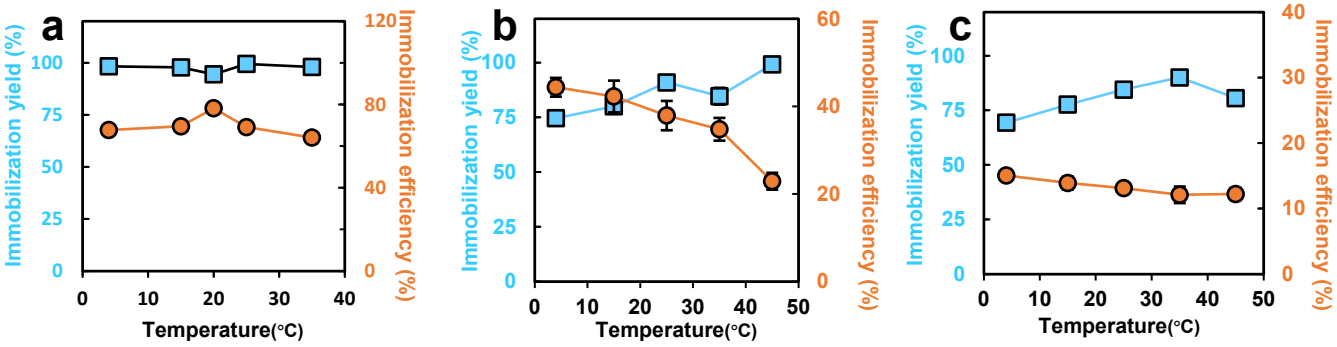

Figure 1. The effect of temperature on the immobilization of enzymes (blue rectangle: immobilization yield, yellow sphere: immobilization efficiency, (**a**) FLS, (**b**) ADH, and (**c**) NOX).

The enzymes are composed of numerous amino acid residues, many of which have acidic or basic side chains. The ionization state of the side chains of enzymes varies at different pH values, and the curve of enzyme activity versus pH is usually shown as a single or double ionization curve [43]. There are two main reasons for this: altering the charged state of the substrate molecule and the enzyme molecule, thus affecting the binding of the enzyme to the substrate; and that a higher or lower pH can affect the stability of the enzyme, which could be irreversibly damaged [44]. In the immobilization step, the pH of the solution would alter the reactivity of the epoxy group on the carrier and the amino acid side chain groups (amino and carboxyl) on the protein [42]. Consequently, we investigated the effect of pH on the immobilization process (Figure 2). The immobilization yields of the three enzymes fluctuated slightly at pH 6–11, and the immobilization yields 75~95% could be obtained. This was mainly attributed to the high reactivity of the epoxide group with the protein side chain moiety [42]. In contrast, the immobilization efficiencies of the three enzymes differed significantly (71% for FLS at pH 7, 41% for ADH at pH 8, and 22% for NOX at pH 9). Notably, ADH lost its catalytic activity at pH 10–11, which may be related to the stability of the enzyme itself. Finally, we chose the pH that obtained the maximum immobilization efficiency as one of the conditions for immobilization.

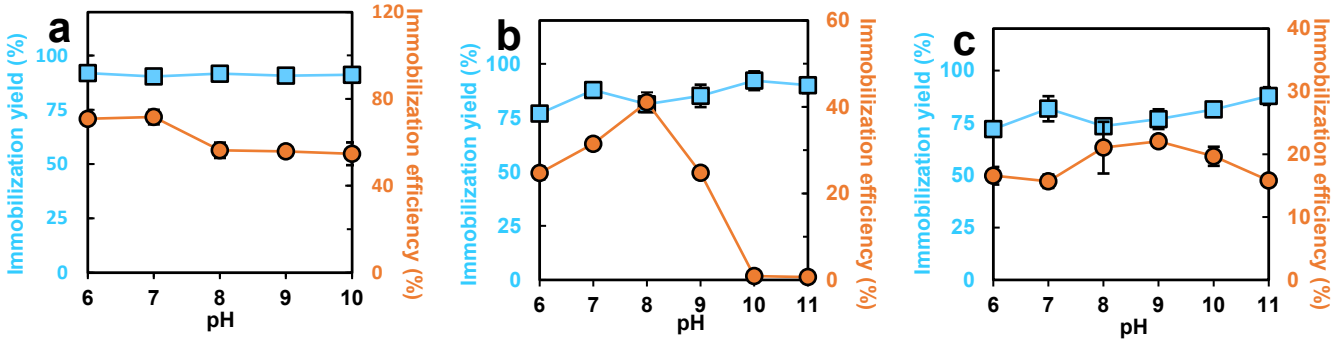

Figure 2. The effect of pH on immobilization (blue rectangle: immobilization yield, yellow sphere: immobilization efficiency, (**a**) FLS, (**b**) ADH, and (**c**) NOX).

3.3. The Effects of the Immobilization Time and the Enzyme Carrier Ratio on the Immobilization

With increasing time, the immobilization yields of ADH and NOX increases, yet the immobilization efficiency declines. This is because the linkage between the enzyme

molecules and epoxy-based modified carriers was facilitated by the increased immobilization time. At the same time, the increase in the immobilization time reinforced the loss of enzyme activity as well [45]. Unlike the previous two enzymes, FLS did not present the expected descent in immobilization yield. This might be related to two causes, the possession of side-chain amino groups with a higher reactivity than FLS and the consistently high apparent immobilization yield due to the adsorption of FLS on the carrier. Physically adsorbed proteins were difficult to count because of their low concentration in the washing solution. Therefore, the immobilization yields for 1 h were significantly lower than the others (Figure 3). Ultimately, 2, 1, and 2 h were determined as the immobilization time for FLS, ADH, and NOX, respectively.

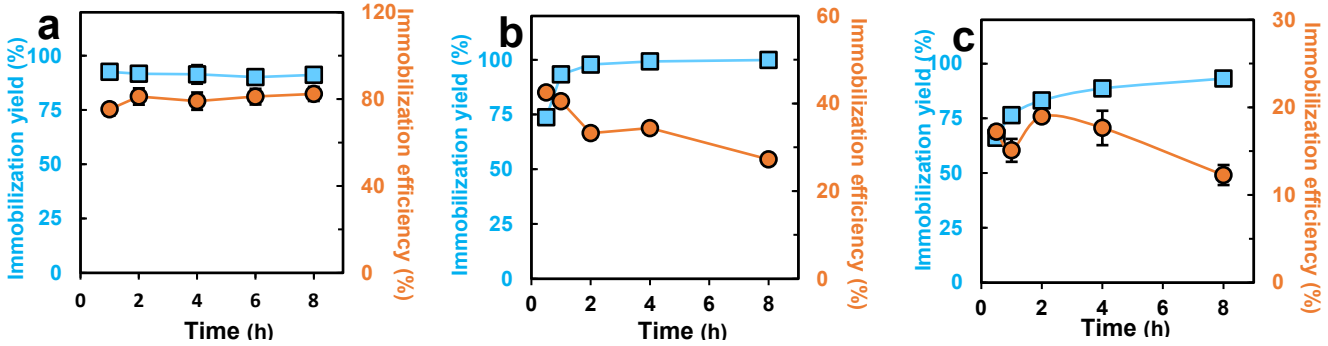

Figure 3. The effect of the immobilization time on the immobilization of enzymes (blue rectangle: immobilization yield, yellow sphere: immobilization efficiency, (**a**) FLS, (**b**) ADH, (**c**) NOX).

The carrier was expected to be able to load as many enzymes as possible for the catalytic reaction, but an excess of enzyme can lead to a thick enzyme shell. This produced severe mass transfer resistance, which caused a loss of enzyme activity [46]. Therefore, the ratio of enzyme to the carrier was also evaluated for a higher immobilization efficiency (Figure 4). The immobilization yields of ADH and NOX increased, yet the efficiency of the immobilization decreased as the amount of enzyme increased. When the ratio of enzyme to carrier exceeded 15, there was a tendency for both the immobilization efficiency and the yield to decrease as the carrier reached its maximum loading capacity. Ultimately, 20, 10, and 10 mg·g^{-1} were selected as the enzyme carrier ratio of FLS, ADH, and NOX, respectively (Figure 4).

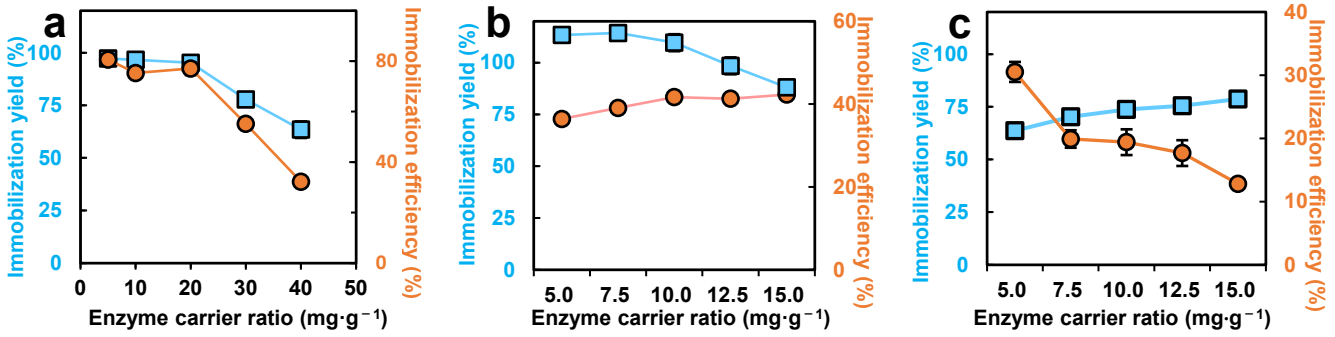

Figure 4. The effect of the ratio of enzymes and carrier on the immobilization of enzymes (blue rectangle: immobilization yield, yellow sphere: immobilization efficiency, (**a**) FLS, (**b**) ADH, and (**c**) NOX).

3.4. The Synthesis of Acetoin with Immobilized Cascade Enzymes and Free Cascade Enzymes

The immobilized enzymes were used to conduct the reaction from ethanol to acetoin under optimized reaction conditions. Figure 5 shows that the conversion of immobilized enzymes was higher than that of free enzymes (59% of conversion), reaching 90% in 45 h with 50 mM ethanol. Under the condition of the same enzyme activity, the immobilized

enzyme with a higher stability than the free enzyme can maintain a higher activity and achieve a higher conversion. In the initial stage of the cascade reaction, the low concentration of the intermediate product acetaldehyde resulted in a slow synthesis rate of acetoin. At this time, it was in the stage of the rapid consumption of ethanol. With the accumulation of acetaldehyde, the synthesis rate of acetoin increases, and finally the three re-reached an equilibrium in the reaction, which was consistent with the results of previous studies [21]. Generally, *engineered E. coli*, *S. cerevisiae*, and *Corynebacterium glutamicum* have been applied for acetoin production with promising results [13–16]. For example, the engineered *Saccharomyces cerevisiae* produced 100.1 g/L acetoin with a yield of 0.44 g/g glucose [17]. The engineered *Corynebacterium glutamicum* produced a titer of 102.45 g/L acetoin with a yield of 0.419 g/g glucose [18]. In addition, there were also studies on the efficient conversion of acetoin by an enzyme cascade or coupling reactions [47,48]. For example, under optimized conditions, α-Acetolactate synthetase (ALS) and α-acetolactate decarboxylase were selected for the synthesis of acetoin using pyruvate [47]. Compared with the production of acetoin by the above methods, the immobilized cascade enzyme has a higher conversion and better operational stability, which indicates its potential in the industrial production of acetoin. This may be mainly attributed to the enhanced enzymatic rigidity of the epoxy-modified magnetic nanomaterials. Magnetic nanomaterials have been applied for the immobilization of various enzymes due to their high activity and low loss for enzyme activity. Likewise, the material can be applied to other synthetic routes of acetoin. The 90% conversion of acetoin has been achieved by immobilizing the cascade enzyme system. However, further optimization of the catalytic conditions and scale-up of the immobilized cascade enzymes at higher substrate concentrations are the next stages of the desired task. In this enzymatic cascade reactions, FLS is the rate-limiting enzyme with the lowest catalytic efficiency. Using rational design or directed evolution to improve the catalytic performance of FLS is urgent research in future work.

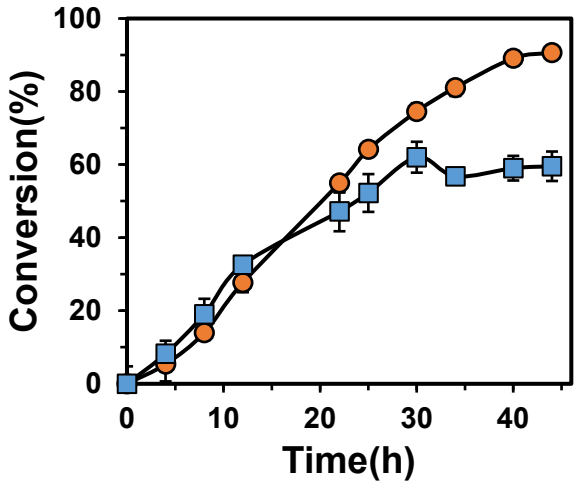

Figure 5. The synthesis of acetoin from ethanol with the immobilized cascade enzymes.

3.5. The Reusability of Immobilized Cascade Enzymes

The economics of industrial and continuous production are related to the reusability of the biocatalysts. Thus, the reusability of the immobilized cascade enzymes was explored through six cycles of reaction (Figure 6). The results showed that the immobilized enzyme exhibited excellent reusability under catalytic conditions when the enzymatic activity of the simultaneously added FLS was higher than that of ADH dehydrogenase. After six reaction batches, the enzyme retained 86.3% of its initial activity. This indicates that the loss of enzyme activity by the intermediate product acetaldehyde can be well reduced by decreasing the substrate concentration and adjusting the enzyme ratio.

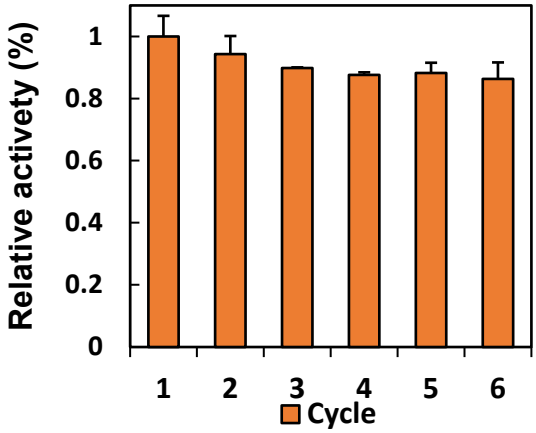

Figure 6. The reusability of the immobilized cascade enzymes.

4. Conclusions

In this work, three well-compatible enzymes (ADH, FLS, and NOX) were screened and immobilized to construct a viable cascade system to transform acetoin. The ADH is used in the conversion of ethanol to acetaldehyde, thus reducing the damage to the enzyme due to the high initial concentration of acetaldehyde. The NOX is designed to reduce the consumption of expensive cofactors and to avoid product inhibition caused by NADH accumulation. The FLS for the conversion of acetaldehyde to acetoin was aimed to avoid the loss of enzyme activity due to the accumulation of acetaldehyde. Immobilization was used to improve the tolerance of the three enzymes to acetaldehyde as well as the stability and reusability of the enzymes. With these results, the immobilized cascade enzymes were able to efficiently convert ethanol to acetoin with a conversion of 90%, indicating that a bioconversion pathway for ethanol upgrading with the potential industrial application has been developed.

Author Contributions: Conceptualization, Y.-W.Z. and P.P.; methodology, X.-Y.L., J.-Y.H. and Y.-W.Z.; software, Y.-Y.X.; validation, J.-Y.H. and Q.Z.; investigation, X.-Y.L., J.-Y.H. and Q.Z.; writing—original draft preparation, X.-Y.L.; writing—review and editing, Y.-W.Z. and P.P.; supervision, Y.-W.Z.; funding acquisition, Y.-W.Z. All authors have read and agreed to the published version of the manuscript.

Funding: This research was funded by Natural Science Foundation of Guangxi Province (2019GXNSFAA185059) and National Natural Science Foundation of China (22068001).

Data Availability Statement: Not applicable.

Conflicts of Interest: The authors declare no conflict of interest.

Abbreviations

ADH	Alcohol dehydrogenase
DTT	Dithiothreitol
FLS	Acetaldehyde lyase
IPTG	Isopropyl-β-D-thiogalactopyranoside
NADH/NAD^+	Reduced nicotinamide adenine dinucleotide
NOX	NADH oxidase
TEOS	Tetraethyl orthosilicate
TPP	Thiamine pyrophosphate
Tris	Tris(hydroxymethyl)methyl aminomethane

References

1. Zhang, Q.; Yang, X.; Guan, J. Applications of magnetic nanomaterials in heterogeneous catalysis. *ACS Appl. Nano Mater.* **2019**, *2*, 4681–4697. [CrossRef]
2. Yilmaz, E.; Sarp, G.; Uzcan, F.; Ozalp, O.; Soylak, M. Application of magnetic nanomaterials in bioanalysis. *Talanta* **2021**, *229*, 122285. [CrossRef]

3. Li, Y.; Wang, X.-Y.; Jiang, X.-P.; Ye, J.-J.; Zhang, Y.-W.; Zhang, X.-Y. Fabrication of graphene oxide decorated with Fe_3O_4@SiO_2 for immobilization of cellulase. *J. Nanopart. Res* **2015**, *17*, 8. [CrossRef]
4. Wang, X.-Y.; Jiang, X.-P.; Li, Y.; Zeng, S.; Zhang, Y.-W. Preparation Fe_3O_4@chitosan magnetic particles for covalent immobilization of lipase from *Thermomyces lanuginosus*. *Int. J. Biol. Macromol.* **2015**, *75*, 44–50. [CrossRef] [PubMed]
5. Xiao, Z.; Lu, J.R. Generation of acetoin and its derivatives in foods. *J. Agric. Food Chem.* **2014**, *62*, 6487–6497. [CrossRef] [PubMed]
6. Li, L.; Wei, X.; Yu, W.; Wen, Z.; Chen, S. Enhancement of acetoin production from bacillus licheniformis by 2,3-butanediol conversion strategy: Metabolic engineering and fermentation control. *Process Biochem.* **2017**, *57*, 35–42. [CrossRef]
7. Xiao, Z.; Lu, J.R. Strategies for enhancing fermentative production of acetoin: A review. *Biotechnol. Adv.* **2014**, *32*, 492–503. [CrossRef]
8. Yang, T.; Rao, Z.; Zhang, X.; Xu, M.; Xu, Z.; Yang, S.-T. Metabolic engineering strategies for acetoin and 2,3-butanediol production: Advances and prospects. *Crit. Rev. Biotechnol.* **2017**, *37*, 990–1005. [CrossRef]
9. Peng, K.; Guo, D.; Lou, Q.; Lu, X.; Cheng, J.; Qiao, J.; Lu, L.; Cai, T.; Liu, Y.; Jiang, H. synthesis of ligustrazine from acetaldehyde by a combined biological–chemical approach. *ACS Synth. Biol.* **2020**, *9*, 2902–2908. [CrossRef]
10. Wang, X.; Lv, M.; Zhang, L.; Li, K.; Gao, C.; Ma, C.; Xu, P. Efficient bioconversion of 2,3-butanediol into acetoin using gluconobacter oxydans DSM 2003. *Biotechnol. Biofuels* **2013**, *6*, 155. [CrossRef]
11. Maina, S.; Prabhu, A.A.; Vivek, N.; Vlysidis, A.; Koutinas, A.; Kumar, V. Prospects on bio-based 2,3-butanediol and acetoin production: Recent progress and advances. *Biotechnol. Adv.* **2022**, *55*, 107783. [CrossRef] [PubMed]
12. Werpy, T.; Petersen, G. *Top Value Added Chemicals from Biomass: Volume I—Results of Screening for Potential Candidates from Sugars and Synthesis Gas*; DOE/GO-102004-1992; National Renewable Energy Laboratory: Golden, CO, USA, 2004; p. 15008859.
13. Lü, C.; Ge, Y.; Cao, M.; Guo, X.; Liu, P.; Gao, C.; Xu, P.; Ma, C. Metabolic engineering of bacillus licheniformis for production of acetoin. *Front. Bioeng. Biotechnol.* **2020**, *8*, 125. [CrossRef] [PubMed]
14. Liu, Z.; Qin, J.; Gao, C.; Hua, D.; Ma, C.; Li, L.; Wang, Y.; Xu, P. Production of (2S,3S)-2,3-butanediol and (3S)-acetoin from glucose using resting cells of *Klebsiella pneumonia* and *Bacillus subtilis*. *Bioresour. Technol.* **2011**, *102*, 10741–10744. [CrossRef] [PubMed]
15. Sun, J.-A.; Zhang, L.-Y.; Rao, B.; Shen, Y.-L.; Wei, D.-Z. Enhanced acetoin production by serratia marcescens H32 with expression of a water-forming nadh oxidase. *Bioresour. Technol.* **2012**, *119*, 94–98. [CrossRef]
16. Wang, M.; Fu, J.; Zhang, X.; Chen, T. Metabolic engineering of bacillus subtilis for enhanced production of acetoin. *Biotechnol. Lett.* **2012**, *34*, 1877–1885. [CrossRef]
17. Lu, L.; Mao, Y.; Kou, M.; Cui, Z.; Jin, B.; Chang, Z.; Wang, Z.; Ma, H.; Chen, T. Engineering Central pathways for industrial-level (3r)-acetoin biosynthesis in corynebacterium glutamicum. *Microb. Cell Factories* **2020**, *19*, 102. [CrossRef]
18. Bae, S.-J.; Kim, S.; Hahn, J.-S. Efficient production of acetoin in saccharomyces cerevisiae by disruption of 2,3-butanediol dehydrogenase and expression of NADH oxidase. *Sci. Rep.* **2016**, *6*, 27667. [CrossRef]
19. Yan, P.; Wu, Y.; Yang, L.; Wang, Z.; Chen, T. Engineering genome-reduced *Bacillus subtilis* for acetoin production from xylose. *Biotechnol. Lett.* **2018**, *40*, 393–398. [CrossRef]
20. Cui, Z.; Wang, Z.; Zheng, M.; Chen, T. Advances in biological production of acetoin: A comprehensive overview. *Crit. Rev. Biotechnol.* **2021**, *93*, 1–22. [CrossRef]
21. Zhang, L.; Singh, R.D.S.; Guo, Z.; Li, J.; Chen, F.; He, Y.; Guan, X.; Kang, Y.C.; Lee, J.-K. An artificial synthetic pathway for acetoin, 2,3-butanediol, and 2-butanol production from ethanol using cell free multi-enzyme catalysis. *Green Chem.* **2018**, *20*, 230–242. [CrossRef]
22. Hohagen, H.; Schwarz, D.; Schenk, G.; Guddat, L.W.; Schieder, D.; Carsten, J.; Sieber, V. Deacidification of grass silage press juice by continuous production of acetoin from its lactate via an immobilized enzymatic reaction cascade. *Bioresour. Technol.* **2017**, *245*, 1084–1092. [CrossRef] [PubMed]
23. Basso, A.; Serban, S. Industrial applications of immobilized enzymes—A review. *Mol. Catal.* **2019**, *479*, 110607. [CrossRef]
24. Bilal, M.; Zhao, Y.; Rasheed, T.; Iqbal, H.M.N. Magnetic nanoparticles as versatile carriers for enzymes immobilization: A review. *Int. J. Biol. Macromol.* **2018**, *120*, 2530–2544. [CrossRef] [PubMed]
25. Jiang, X.-P.; Lu, T.-T.; Liu, C.-H.; Ling, X.-M.; Zhuang, M.-Y.; Zhang, J.-X.; Zhang, Y.-W. Immobilization of dehydrogenase onto epoxy-functionalized nanoparticles for synthesis of (R)-mandelic acid. *Int. J. Biol. Macromol.* **2016**, *88*, 9–17. [CrossRef] [PubMed]
26. Li, F.-L.; Shi, Y.; Zhang, J.-X.; Gao, J.; Zhang, Y.-W. Cloning, expression, characterization and homology modeling of a novel water-forming NADH oxidase from *Streptococcus mutans* ATCC 25175. *Int. J. Biol. Macromol.* **2018**, *113*, 1073–1079. [CrossRef]
27. Behling, R.; Valange, S.; Chatel, G. Heterogeneous Catalytic oxidation for lignin valorization into valuable chemicals: What results? What limitations? What trends? *Green Chem.* **2016**, *18*, 1839–1854. [CrossRef]
28. Siegel, J.B.; Smith, A.L.; Poust, S.; Wargacki, A.J.; Bar-Even, A.; Louw, C.; Shen, B.W.; Eiben, C.B.; Tran, H.M.; Noor, E.; et al. Computational protein design enables a novel one-carbon assimilation pathway. *Proc. Natl. Acad. Sci. USA* **2015**, *112*, 3704–3709. [CrossRef]
29. Bradford, M.M. A rapid and sensitive method for the quantification of microgram quantities of protein utilizing the principle of protein-dye binding. *Anal. Biochem.* **1976**, *72*, 248–254. [CrossRef]
30. Zhuang, M.-Y.; Jiang, X.-P.; Ling, X.-M.; Xu, M.-Q.; Zhu, Y.-H.; Zhang, Y.-W. Immobilization of glycerol dehydrogenase and NADH oxidase for enzymatic synthesis of 1,3-dihydroxyacetone with in situ cofactor regeneration: Enzymatic production of 1, 3-dihydroxyacetone via immobilized enzymes. *J. Chem. Technol. Biotechnol.* **2018**, *93*, 2351–2358. [CrossRef]

31. Nisar, M.A.; Rashid, N.; Bashir, Q.; Gardner, Q.-A.A.; Shafiq, M.H.; Akhtar, M. TK1299, a highly thermostable NAD(P)H oxidase from *Thermococcus kodakaraensis* exhibiting higher enzymatic activity with NADPH. *J. Biosci. Bioeng.* **2013**, *116*, 39–44. [CrossRef]
32. Palma-Gutiãrez, H.N.; Rodrãguez-Zavala, J.S.; Jasso-Chãvez, R.; Moreno-Sãnchez, R.; Saavedra, E. Gene Cloning and Biochemical Characterization of an Alcohol Dehydrogenase from *Euglena gracilis*. *J. Eukaryot. Microbiol.* **2008**, *55*, 554–561. [CrossRef] [PubMed]
33. Gao, H.; Tiwari, M.K.; Kang, Y.C.; Lee, J.-K. Characterization of H_2O-forming NADH Oxidase from *Streptococcus pyogenes* and its application in l-rare sugar production. *Bioorganic Med. Chem. Lett.* **2012**, *22*, 1931–1935. [CrossRef] [PubMed]
34. Zhang, Y.-W.; Tiwari, M.K.; Gao, H.; Dhiman, S.S.; Jeya, M.; Lee, J.-K. Cloning and characterization of a thermostable H_2O-forming NADH oxidase from *Lactobacillus rhamnosus*. *Enzym. Microb. Technol.* **2012**, *50*, 255–262. [CrossRef] [PubMed]
35. Li, F.-L.; Su, W.B.; Tao, Q.-L.; Zhang, L.-Y.; Zhang, Y.-W. Expression, biochemical characterization, and mutation of a water forming NADH: FMN oxidoreductase from *Lactobacillus rhamnosus*. *Enzym. Microb. Technol.* **2020**, *134*, 109464. [CrossRef]
36. Kawasaki, S.; Ishikura, J.; Chiba, D.; Nishino, T.; Niimura, Y. Purification and characterization of an H_2O-forming NADH oxidase from *Clostridium aminovalericum*: Existence of an oxygen-detoxifying enzyme in an obligate anaerobic bacteria. *Arch. Microbiol.* **2004**, *181*, 324–330. [CrossRef]
37. Ma, M.; Wang, X.; Zhang, X.; Zhao, X. Alcohol dehydrogenases from scheffersomyces stipitis involved in the detoxification of aldehyde inhibitors derived from lignocellulosic biomass conversion. *Appl. Microbiol. Biotechnol.* **2013**, *97*, 8411–8425. [CrossRef]
38. Nie, Y.; Xu, Y.; Mu, X.Q.; Wang, H.Y.; Yang, M.; Xiao, R. Purification, characterization, gene cloning, and expression of a novel alcohol dehydrogenase with anti-prelog stereospecificity from *Candida parapsilosis*. *Appl. Environ. Microbiol.* **2007**, *73*, 3759–3764. [CrossRef]
39. Cao, Y.; Liao, L.; Xu, X.; Oren, A.; Wang, C.; Zhu, X.; Wu, M. Characterization of alcohol dehydrogenase from the Haloalkaliphilic Archaeon *Natronomonas pharaonis*. *Extremophiles* **2008**, *12*, 471–476. [CrossRef]
40. Timpson, L.M.; Alsafadi, D.; Mac Donnchadha, C.; Liddell, S.; Sharkey, M.A.; Paradisi, F. Characterization of alcohol dehydrogenase (ADH12) from *Haloarcula marismortui*, an Extreme halophile from the dead sea. *Extremophiles* **2012**, *16*, 57–66. [CrossRef]
41. De María, P.D.; Stillger, T.; Pohl, M.; Wallert, S.; Drauz, K.; Gröger, H.; Trauthwein, H.; Liese, A. Preparative enantioselective synthesis of benzoins and (r)-2-hydroxy-1-phenylpropanone using benzaldehyde lyase. *J. Mol. Catal. B Enzym.* **2006**, *38*, 43–47. [CrossRef]
42. Fraenkel-Conrat, H. The action of 1,2-epoxides on proteins. *J. Biol. Chem.* **1944**, *154*, 227–238. [CrossRef]
43. Bearne, S.L. Illustrating the effect of pH on enzyme activity using gibbs energy profiles. *J. Chem. Educ.* **2014**, *91*, 84–90. [CrossRef]
44. Chaloupkova, R.; Prokop, Z.; Sato, Y.; Nagata, Y.; Damborsky, J. Stereoselectivity and conformational stability of haloalkane dehalogenase dbja from *Bradyrhizobium japonicum* USDA110: The effect of pH and temperature: Stereochemistry and conformational stability of DbjA. *FEBS J.* **2011**, *278*, 2728–2738. [CrossRef] [PubMed]
45. Xu, M.-Q.; Li, F.-L.; Yu, W.-Q.; Li, R.-F.; Zhang, Y.-W. Combined cross-linked enzyme aggregates of glycerol dehydrogenase and NADH oxidase for high efficiency in situ NAD^+ regeneration. *Int. J. Biol. Macromol.* **2020**, *144*, 1013–1021. [CrossRef]
46. Benítez-Mateos, A.I.; Huber, C.; Nidetzky, B.; Bolivar, J.M.; López-Gallego, F. Design of the enzyme–carrier interface to overcome the O_2 and NADH mass transfer limitations of an immobilized flavin oxidase. *ACS Appl. Mater. Interfaces* **2020**, *12*, 56027–56038. [CrossRef]
47. Cui, Z.; Mao, Y.; Zhao, Y.; Zheng, M.; Wang, Z.; Ma, H.; Chen, T. One-Pot efficient biosynthesis of (3R)-acetoin from pyruvate by a Two-Enzyme cascade. *Catal. Sci. Technol.* **2020**, *10*, 7734–7744. [CrossRef]
48. Cui, Z.; Zhao, Y.; Mao, Y.; Shi, T.; Lu, L.; Ma, H.; Wang, Z.; Chen, T. In Vitro biosynthesis of optically pure D—(−)—Acetoin from meso-2,3-butanediol using 2,3-butanediol dehydrogenase and NADH oxidase. *J. Chem. Technol. Biotechnol.* **2019**, *94*, 2547–2554. [CrossRef]